

# Real-Time Charge Oscillation between Monomers in a Dimeric System Associated with Intermolecular Vibration Induced by an Ultrashort Pulse

Takayoshi Kobayashi\* and Masakatsu Hirasawa

Department of Physics, Graduate School of Science, The University of Tokyo, 7-3-1 Hongo, Bunkyo, Tokyo 113-0033, Japan

Received: May 25, 2004; In Final Form: September 30, 2004

Ultrafast charge resonant (CR) dynamics between two molecules in a dimer system has been studied theoretically and experimentally using 6-fs laser pulses and a thin film of amorphous-phase phthalocyanine tin(IV) dichloride (SnPc). The modulation of the absorbance change in the bleaching spectral range of the CR absorption band was analyzed to obtain the amount of charge resonantly transferred back and forth by a dimeric vibration induced by photoexcitation. The modulation can be explained in terms of a periodic change in the cross section and a periodic energy shift, where both are induced by the change in the overlap integral caused by the accordion-type intermolecular vibration. The associated change in distance between two molecules with the intermolecular vibration was estimated to be 0.09 Å, which corresponds to 2.5% of the mean distance between the two SnPc molecules in the dimeric system.

## 1. Introduction

Charge resonance (CR) is a widely found phenomenon in single molecule systems, molecular systems, and solid-state materials with a mirror symmetry or an inversion symmetry. A most fundamental example of the first systems is a benzene molecule, which has canonical (resonant) Kekule structures<sup>1</sup> with two different quantum mechanical resonant configurations with three double bonds and three single bonds. In such system the  $\pi$ -electron is considered to be resonantly transferred between neighboring C–C bonds. Also among three types of canonical Dewar benzene,<sup>1</sup> the charges are transferred from one of the three bonds connecting the diagonal carbons. The most typical and interesting example among the second systems is an “excimer”<sup>4</sup> originally named from an excited dimer. Efficient bidirectional charge transfer between like molecules in the excimer and stabilization due to the resonance between the transfer of electrons in opposite directions takes place only in the excited state because of the enhanced overlap of  $\pi$ -electrons resulting from the extended electron distributions in each component. The  $\pi$ -electron overlap between the two component molecules in the ground state is too small to allow the efficient charge resonance to take place to stabilize the stable dimer configuration and the two components are repulsive. Examples of the third systems can be found in varieties of complex systems such as organic molecular crystals of macrocyclic rings<sup>2</sup> of two-dimensionally extended  $\pi$ -electrons and also in mixed-valence systems with a quasi-one-dimensionality.<sup>3</sup> In some cases, the word “charge transfer” (CT) is sometimes used for charge resonance (CR). Charge-transfer means a unidirectional electron transfer under a more strict definition.

In this paper we chose a metal phthalocyanine (MPc) complex, phthalocyanine tin(IV) dichloride (SnCl<sub>2</sub>Pc), which is known to have a dimeric structure similar to that in PbPc<sup>5</sup>, as a sample to show real-time observation of charge resonance coupled to an intermolecular vibration. Pc is a nonlinear optical organic material that has been studied for its potential capabilities

for all-optical devices such as optical switches and optical limiters.<sup>6,7</sup> A good example of demonstration of the applicability was made using thin films of SnCl<sub>2</sub>Pc.<sup>7</sup>

## 2. Experimental Section

**2.1. Sample.** A thin film sample of phthalocyanine tin(IV) dichloride (SnPc) was prepared by vacuum evaporation in base pressure  $1.6 \times 10^{-5}$  Torr on a 1-mm-thick glass substrate. The sample thickness measured using a surface-roughness tester (SurfTest SV-400; Mitutoyo Corp.) ranged between 200 and 400 nm between two ends with nearly constant inclination. The evaporated thin film of SnPc is supposed to be in an amorphous phase<sup>8</sup> with so-called “shuttlecock-shaped” molecules stacked normal to the molecular planes in one-dimensional columns.<sup>9</sup> Precise measurement was carried out for stationary absorption and the spectrum was deconvoluted to the locally excited Q<sub>X</sub>-, and Q<sub>Y</sub>-bands together with the CT band in our previous report.<sup>10</sup>

**2.2. 6-fs NOPA for Real-Time Spectroscopy.** The 6-fs pulsed light source and the setup for femtosecond time-resolved absorption spectroscopy were shown in Figure 1, which was previously described in detail.<sup>11–14</sup> The 6-fs, 1-kHz pulse train was generated from the noncollinear optical parametric amplifier (NOPA) with a pulse compressor using a flexible mirror,<sup>11,12</sup> of which the wavelength range extends from 500 to 750 nm. The pulse energies (intensities) of the pump and probe at the sample position were about 20 and 5 nJ, respectively, corresponding to photon numbers of  $7.5 \times 10^{14}$  and  $8.5 \times 10^{13}$  photon/cm<sup>2</sup>, respectively. To detect the pump–probe signals at various wavelengths simultaneously, we employed a 128-channel multichannel double lock-in amplifier with 128 avalanche photodiodes (APDs). The probe signals spectrally resolved by a polychromator (JASCO M25-TP) were detected by the APDs. The signals from the APDs are analyzed by the multi-lock-in amplifier simultaneously with the reference frequency of a mechanical chopper (230 Hz). The absorbance changes in the 500–720 nm region were measured for the delay time range between –0.5 and 4 ps with a 2.5 fs interval.

\* Corresponding author: Phone: +81-3-3841-4227. Fax: +81-3-3841-4165. E-mail: kobayashi@phys.s.u-tokyo.ac.jp.

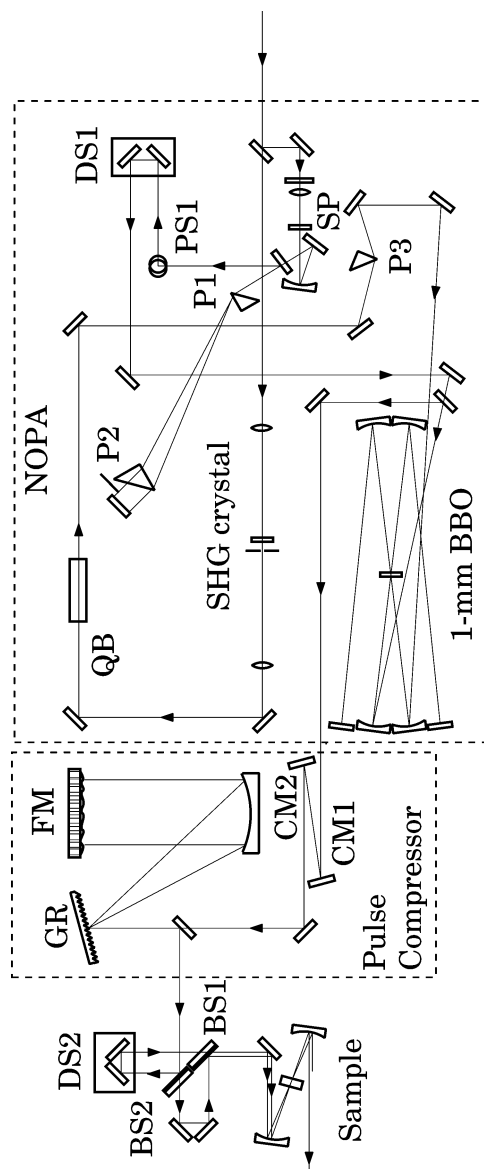


**Figure 1.** Schematic of experimental setup. The double-pass noncollinear optical parametric amplifier (NOPA) was excited by the 120-fs, 0.15-mJ 780-nm output from Ti:sapphire REGEN amplifier at 1 kHz. The chirp of the NOPA output was compensated by the pulse compressor consisting of a chirped mirror pair (CM1, CM2), a grating (GR), and a flexible mirror (FM).

### 3. Results and Discussion

**3.1. Experimental Results.** Figure 2 shows several examples of the real-time traces of the absorbance change ( $\Delta A$ ) induced by 6-fs laser pulse excitation. The figure covers the spectral range 556–665 nm ( $15000$ – $18000$   $\text{cm}^{-1}$ ). The signal of the absorbance change was integrated over a spectral width of 16 nm. In the spectral range between 550 and 600 nm, which well overlaps with the CR excitation region, the signals do not decay substantially up to 4 ps. The lifetime was previously reported<sup>15</sup> to be longer than one nanosecond and at shorter delay time it decays slightly because of exciton–exciton interaction induced by the Auger process as discussed in our previous paper.<sup>16</sup>

Figure 3 exhibits the Fourier transforms of the real-time traces shown in Figure 2. All of the Fourier power spectra exhibit several commonly observed frequency components with different intensity distribution profiles depending on the probe photon energy. In our previous paper,<sup>10</sup> the corresponding contour map for 6-fs pulse excitation was shown in the electronic

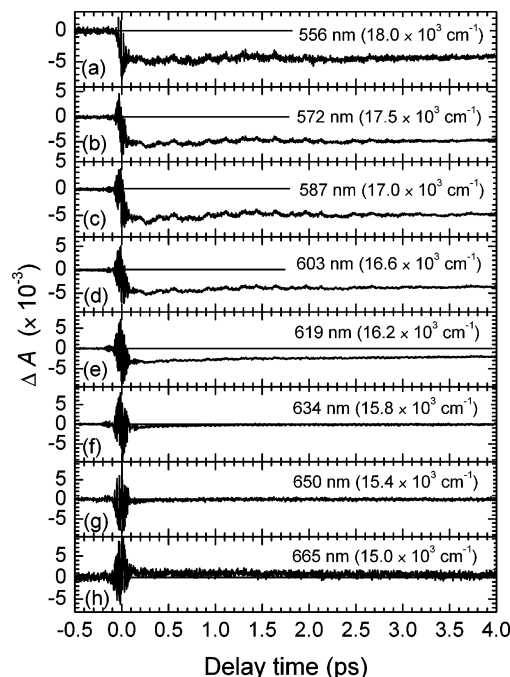


**Figure 2.** (a–h) Delay time traces of absorbance change of SnPc thin film after being excited with 6-fs pulses. The spectra were averaged over five channels, resulting in a spectral resolution of 15 nm.

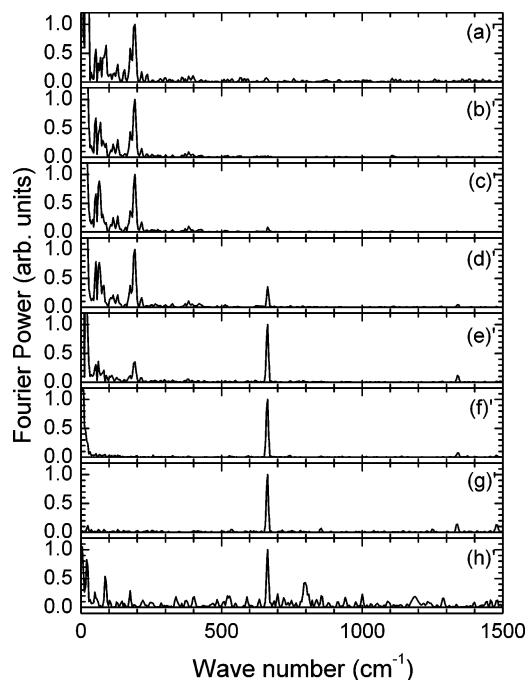


**Figure 3.** (a'–h') Fourier power spectra of the absorbance change of SnPc thin film calculated from the time traces (a–h) in Figure 2 between 0.2–4 ps.

spectral and vibrational frequency regions of 550–660 nm ( $15150$ – $18200$   $\text{cm}^{-1}$ ) and  $100$ – $2000$   $\text{cm}^{-1}$ . It can be seen that there are Fourier components due to intermolecular or intramolecular vibrations with mode frequencies of 190, 670, and  $1340$   $\text{cm}^{-1}$ . They were assigned as an accordion-type intermolecular vibration,  $B_{1g}$  macrocycle deformation, and the first overtone (the second harmonic) of the  $B_{1g}$  macrocycle deformation ( $670$   $\text{cm}^{-1}$ ), respectively.<sup>17</sup> The figure shows that the mode of  $670$   $\text{cm}^{-1}$  has large power at the locally excited transition (Q-band), which is the main near-infrared absorption band in Pc's. On the other hand, the  $190$   $\text{cm}^{-1}$  mode has large power around the

CR transition (16700 cm<sup>-1</sup>), which was discussed in our previous paper.<sup>10</sup> Here we concentrate on the 190 cm<sup>-1</sup> mode.

**3.2. Theoretical Considerations.** The wave functions after configuration interaction (CI) of the electronic states of AB dimers of like molecules in the ground state  $|G\rangle$  and an excited state can be described as linear combinations of several electronic states before CI. The wave functions before CI are the ground state  $|G^0\rangle$ , charge-transfer states  $|CT^A\rangle \equiv |A^+B^- \rangle$  and  $|CT^B\rangle \equiv |A^-B^+ \rangle$ , and the locally excited states  $|LE^A\rangle \equiv |A^*B\rangle$  and  $|LE^B\rangle \equiv |AB^*\rangle$ . After CI, the ground  $|G\rangle$  and the charge resonance excited state  $|E\rangle$  can be linear combinations of them.<sup>18,19</sup>

$$|G\rangle = a|G^0\rangle + \sum_i (B_i|A^+B^- \rangle + C_i|A^-B^+ \rangle + D_i|A^*B\rangle + E_i|AB^*\rangle) \quad (1)$$

$$|E\rangle = a'|G^0\rangle + \sum_i (B'_i|A^+B^- \rangle + C'_i|A^-B^+ \rangle + D'_i|A^*B\rangle + E'_i|AB^*\rangle) \quad (2)$$

Among the coefficients in eq 1  $|a|$  is the largest and  $|B'_i|$  or  $|C'_i|$  is the largest in eq 2. Then the charge-resonant (CR) states  $|CR^+\rangle$  and  $|CR^-\rangle$  and two exciton-coupling state  $|EC^*\rangle$  are defined as follows.

$$|G\rangle = a|G^0\rangle + \sum_i (b_i|CR^+\rangle + c_i|CR^-\rangle + d_i|EC^+\rangle + e_i|EC^-\rangle) \quad (3)$$

$$|E\rangle = a'|G^0\rangle + \sum_i (b'_i|CR^+\rangle + c'_i|CR^-\rangle + d'_i|EC^+\rangle + e'_i|EC^-\rangle) \quad (4)$$

$$|CR^+\rangle = \frac{1}{\sqrt{2}}(|CT^A\rangle + |CT^B\rangle) \quad (5a)$$

$$|CR^-\rangle = \frac{1}{\sqrt{1}}(|CT^A\rangle - |CT^B\rangle) \quad (5b)$$

$$|EC^+\rangle = \frac{1}{\sqrt{2}}(|LE^A\rangle + |LE^B\rangle) \quad (6a)$$

$$|EC^-\rangle = \frac{1}{\sqrt{2}}(|LE^A\rangle - |LE^B\rangle) \quad (6b)$$

$$|CT^A\rangle = |\theta_A^{-1}\phi_B\rangle \quad (7a)$$

$$|CT^B\rangle = |\phi_A\theta_B^{-1}\rangle \quad (7b)$$

$$|LE^A\rangle = |\theta_A^{-1}\phi_A\rangle \quad (8a)$$

$$|LE^B\rangle = |\theta_B^{-1}\phi_B\rangle \quad (8b)$$

Here  $\theta$  is the highest occupied molecular orbital (HOMO) and  $\phi$  is the lowest unoccupied molecular orbital (LUMO) in one of the molecules. In the above expression it is assumed that the dimer system has a mirror or inversion symmetry.

$$|\theta_A\rangle = \sum_p f_p^A |\chi_p^H\rangle \quad (9a)$$

$$|\phi_B\rangle = \sum_q f_q^B |\chi_q^L\rangle \quad (9b)$$

where  $|\chi_p^H\rangle$  is the atomic orbital (AO) of atom  $p$  in HOMO, and  $|\chi_q^L\rangle$  is the atomic orbital of atom  $q$  in LUMO.

The transition dipole moments between the ground state  $|G^0\rangle$  and the CR excited  $|CT^+\rangle$  and  $|CT^-\rangle$  state can be calculated, and from the value between  $|G^0\rangle$  state and  $|CT^A\rangle$  state transition dipole moments can also be calculated in the following way<sup>20</sup> by utilizing the Mulliken approximation.<sup>21</sup>

$$\begin{aligned} \langle G^0|\mu|CT^+\rangle &= \frac{1}{\sqrt{2}}(\langle G^0|\mu|CT^A\rangle + \langle G^0|\mu|CT^B\rangle) \\ &= \sqrt{2} \sum_{p,q} g_p^A g_q^B \int \chi_p(1) \mu \chi_q(1) d\tau_1 + \\ &\quad \sqrt{2} \sum_{p,q} g_p^B g_q^A \int \chi_p(1) \mu \chi_q(1) d\tau_1 \\ &\cong \sqrt{2} \sum_{p,q} g_p^A g_q^B [(R_p - R_q) S_{p,q}] \end{aligned} \quad (10a)$$

$$\langle G^0|\mu|CT^-\rangle \cong 0 \quad (10b)$$

$$\begin{aligned} \langle G^0|\mu|LE^A\rangle &= \frac{1}{\sqrt{2}}\langle \theta_A|\mu|\phi_A\rangle = \frac{1}{\sqrt{2}}\langle \theta_B|\mu|\phi_B\rangle = \\ &\quad \frac{1}{\sqrt{2}}\langle G|\mu|LE^B\rangle \end{aligned} \quad (11)$$

$$\langle G^0|\mu|EC^+\rangle \cong \sqrt{2}\langle \theta|\mu|\phi\rangle \quad (12a)$$

$$\langle G^0|\mu|EC^-\rangle \cong 0 \quad (12b)$$

$$\begin{aligned} \langle G|\mu|CT^A\rangle &= \frac{1}{\sqrt{2}}\langle G|\mu|A^+B^- \rangle = \sqrt{2} \sum_{p,q} f_p^A f_q^B \langle \chi_p^H|\mu|\chi_q^L\rangle \\ &\cong \sqrt{2}e \sum_{p,q} f_p^A f_q^B (R_p - R_q) S_{p,q}/2 \end{aligned} \quad (13)$$

Here  $S_{p,q}$  is the overlap integral between two atomic orbitals  $|\chi_p\rangle$  and  $|\chi_q\rangle$  belonging to molecules A and B, respectively.

$$S_{p,q} \equiv \int \chi_p(1) \chi_q(1) d\tau_1, R_p = \langle \chi_p|r|\chi_p\rangle$$

Because of the symmetry of the dimer system, the following are satisfied.

$$\langle G^0|\mu|CR^+\rangle = 0 \quad (14a)$$

$$\langle G^0|\mu|CR^-\rangle = \sqrt{2}e \sum_{p,q} f_p^A f_q^B (R_p - R_q) S_{p,q} \quad (14b)$$

$$\langle LE^A|\mu|CT^A\rangle = -\langle LE^B|\mu|CT^B\rangle \cong 0 \quad (15)$$

$$\langle CT^A|\mu|CT^B\rangle = \langle CT^B|\mu|CT^A\rangle \cong 0 \quad (16)$$

Also from the symmetry of the dimer system

$$\langle CT^A|\mu|CT^A\rangle \cong -\langle CT^B|\mu|CT^B\rangle \cong e(R_B - R_A) \quad (17)$$

Here  $e$  is the electron charge and  $R_A$  and  $R_B$  are the coordinates of the centers of molecules A and B. Therefore, the diagonal elements of the dipole moment in the dimer system with the assumed symmetry of sandwich structure disappear as follows.

$$\langle CR^+|\mu|CR^+\rangle \cong \langle CR^-|\mu|CR^-\rangle \cong 0 \quad (18)$$

$$\langle CR^+|\mu|CR^-\rangle \cong \langle CR^-|\mu|CR^+\rangle \cong 0 \quad (19)$$

Also  $\langle CR^+|\mu|LE^+\rangle$ ,  $\langle CR^+|\mu|LE^-\rangle$ ,  $\langle CR^-|\mu|LE^-\rangle$ , and

$\langle CR^-|\mu|LE^+ \rangle$  are all negligibly small because they are three-center or four-center integrals.

Then the transition moment from the ground state  $|G\rangle$  and the charge-resonance state  $|E\rangle$  after the configuration interaction is given as follows.

$$\begin{aligned} \langle E|\mu|G \rangle &= (ac'^* + a'^*c)\langle CRq^-|\mu|G^0 \rangle + \\ &\quad (ad'^* + a'^*d)\langle EC^+|\mu|G^0 \rangle \\ &= \sqrt{2} \sum_{p,q} \{ (ac'^* + a'^*c)g_p^A g_q^B + \\ &\quad (ad'^* + a'^*d)g_p^A g_q^B \} [(R_p - R_q)S_{pq}] \quad (20) \end{aligned}$$

**3.3. Effect of Molecular Vibrations on the Transition Dipole Moment to CR State.** The most efficiently contributing terms in eq 20 are those with the large atomic orbital overlap integrals among many pairs of  $S_{pq}$  between the atomic orbital  $|p\rangle$  belonging to molecule A and the atomic orbital  $|q\rangle$  belonging to atom B. If it is assumed that the dimers have the sandwich-type structure, the  $S_{pq}$  has the largest overlap between the corresponding atoms belonging to the two molecules to be the mean interplanar distance between the two. For all pairs of  $(p, q)$

$$S_{pq} \approx S_{AB} = f(R_p - R_q) \quad (21)$$

The overlap integral is given approximately exponential function and hence it is sensitive to the distance between the molecules A and B. During the period of intermolecular vibrational motion, the mean distance between the molecules forming the dimer-like configuration varies. The effect of the variation of the distance  $R_p - R_q$  on the dipole moment given by eq 20 can be disregarded, while  $S_{pq}$ , which can be most simply represented with an exponential function, can substantially modify the dipole moment. We can neglect the small change in the linear terms of  $R_A - R_B$  due to accordion-type intermolecular vibration in comparison with that in the  $S_{AB}$  terms. The modulation of the probability  $P$  of transition from the ground state to the CR state intermolecular vibration impulsively excited by ultrashort resonant pulse is calculated in the following way. Equation 20 can be approximated as follows.

$$\langle E|\mu|G \rangle = AS_{AB} \quad (22)$$

The average overlap integral  $S_{AB}$  for the PC molecular dimer system is supposed to have the following approximate dependence on the intermolecular separation  $R$ ,

$$S_{AB} = S_{AB}(0)e^{-R/R_0} \quad (23)$$

Here  $R_0$  is approximated to be 3.6 Å from the 2p orbital of carbon atoms. From the X-ray diffraction analysis<sup>5</sup> the mean distance  $R_{av}$  of the molecular dimer system is estimated to be 3.35 Å for the PbPc. This value was used for SnPc because of the structural similarity between them and also the discussion to be made is not much affected by the difference in  $R_{av}$ .

In the following, the pump-probe data are analyzed in terms of vibrational modulation of transient spectrum. The transient spectrum  $S(\omega)$  is assumed to be modulated as  $S'(\omega)$  by change in the intensity and transition energy with molecular vibrational frequency  $\Omega$  as follows.

$$S'(\omega) = S(\omega - \delta\omega(t))(1 + \delta\alpha(t)) \quad (24)$$

Here amplitude change and energy shift,  $\delta\alpha(t)$  and  $\delta\omega(t)$  are

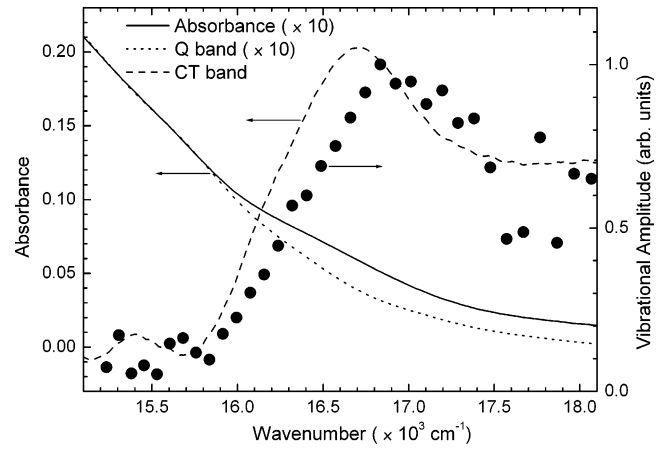


**Figure 4.** Fourier amplitude spectra of the vibrational modes of 190  $\text{cm}^{-1}$  (solid circles). Absorption spectra (solid curve), the CT-band (dashed curve), and the Q-band (dotted curve) are also shown.

respectively given as

$$\delta\alpha(t) = \delta\alpha \cos \Omega t = (\delta(\mu^2)/\mu^2) \cos \Omega t \quad (25)$$

$$\delta\omega(t) = \delta\omega \cos \Omega t \quad (26)$$

The modulation frequency,  $\Omega$ , corresponds to 190  $\text{cm}^{-1}$  of accordion-type intermolecular vibration. Equation 24 can be approximated as

$$\begin{aligned} S'(\omega) &\approx S(\omega) + \left( \delta S(\omega) - \delta\omega \frac{dS(\omega)}{d\omega} \right) \cos \Omega t \\ &\equiv S_{\text{slow}}(\omega) + S_{\text{osc}}(\omega) \cos \Omega t \quad (27) \end{aligned}$$

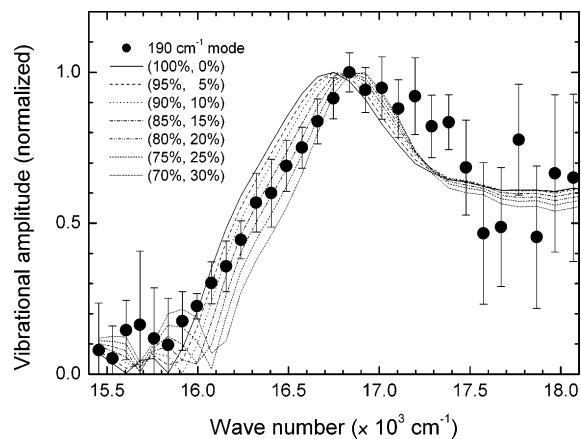
This means that the modulated spectrum  $S'(\omega)$  is composed of slow component  $S_{\text{slow}}(\omega)$  due to the electronic transition and rapidly oscillating component  $S_{\text{osc}}$  that is caused by molecular vibration impulsively excited by the short-pulse excitation. The slow-component spectrum  $S_{\text{slow}}(\omega)$  in the CR absorption range was well analyzed in terms of absorption saturation in our previous paper.<sup>10</sup>

Figure 4 shows the absorption spectrum of Pc and the separated spectra into Q-band (sum of  $Q_X$  and  $Q_Y$  band) and CT bands. The figure also shows the amplitude spectra of the slow and oscillating components,  $S_{\text{slow}}(\omega)$  and  $S_{\text{osc}}(\omega)$ , respectively. As expected from eq 27, the modulated spectrum  $S_{\text{osc}}(\omega)$  can be simulated with the sum of the contribution of  $S_{\text{slow}}(\omega)$  and its frequency derivative  $dS_{\text{slow}}(\omega)/d\omega$ . Their values provide the sizes of the contributions from the absorbance change which are proportional to the change in the squared transition dipole moment and the energy shift. The contribution from the absorbance change is the term representing the deviation from the Condon approximation, which is reported for many fields: nonradiative relaxation,<sup>22</sup> Raman intensity,<sup>23</sup> long-range electron transfer,<sup>24</sup> and electronic transition in the condensed phase.<sup>25</sup> The ratio between the modulated with sine function and unmodulated transition probabilities by molecular vibration of small amplitude of  $\delta R$  can be given by

$$\frac{\delta P}{P} = \frac{\delta(|\langle E|\mu|G \rangle|^2)}{|\langle E|\mu|G \rangle|^2} = 2 \frac{\delta S_{AB}}{S_{AB}} = -2 \frac{\delta R}{R_0} \quad (28)$$

From the experimental results of the modulation of absorbance  $\Delta A$  (which is proportional to  $\delta P/P$ ) being 0.05 at the probe wavelength of 587 nm,  $\delta R$  is determined to be 0.09 Å. The





**Figure 5.** Simulated vibration amplitude for various parameters of contribution from the first and the second terms in eq 27. Solid dots show the normalized vibrational amplitude of the modes  $190\text{ cm}^{-1}$ .

fraction of the modulation of mean distance,  $\delta R/R_{av}$ , is then calculated to be about 2.5%.

There are two contributions in the energy derivative type dependence which causes energy shift. The first one is most popularly observed in many experiments and is due to the wave packet motion either in the ground state or in the excited state.<sup>26</sup> Because the phase of the modulation observed is a nearly cosine function and the phase shift was estimated to be smaller than  $\pi/6$ , it can be considered mainly due to the ground-state wave packet. It is also justified that stationary absorption intensity in the spectral range is weaker than that of  $Q_Y$ - and  $Q_X$ -bands but it is still intense enough for the difference transmittance signal to be positive (bleaching). The second term in the parentheses in eq 27 is due to the changing electronic excitation energy induced by changing the mixing of electronic state as discussed earlier in the present paper.

Figure 5 shows that the simulation of modulated spectrum represented by eq 27 with the relative fractions of the first and the second terms being used as fitting parameters. The fractions of the former and the latter were set to be (70%, 30%), (75%, 25%), (80%, 20%), (85%, 15%), (90%, 10%), (95%, 5%), and (100%, 0%). The (75%, 25%) gives the best fit as seen from Figure 5, and the contribution of the derivative is estimated to be  $25 \pm 5\%$ . There is deviation between the experimental result and the fitted curve at frequencies higher than  $17.0 \times 10^3\text{ cm}^{-1}$  and at frequencies lower than  $16.3 \times 10^3\text{ cm}^{-1}$ . The most essential point is the fact that the peak amplitude of  $190\text{ cm}^{-1}$  is obtained by the  $25 \pm 5\%$  contribution of the energy shift.

The ratio of modulation amplitude of the transition probability against slow absorbance change  $S_{osc}(\omega)/S_{slow}(\omega)$  was estimated to be 0.05. From the relation

$$\frac{\delta P}{P} = \frac{S_{osc}(\omega)}{S_{slow}(\omega)} \quad (29)$$

and eq 24, the change of the mean intermolecular distance between monomers in a dimer system is estimated as  $|\delta R/R_0| = 0.05$ , and hence  $|\delta R| \cong 0.09\text{ \AA}$ . The first excited vibrational level of the mode with the frequency of  $190\text{ cm}^{-1}$  of the intermolecular vibration is incoherently populated at room temperature. The vibrational amplitude for a simple one-dimensional Harmonic oscillator is given by

$$\langle x \rangle = \hbar \sqrt{\frac{2E_{vib}}{m\hbar^2\Omega^2}} \quad (30)$$

Here  $E_{vib}$  and  $m$  are the energy of the vibration and the reduced molecular mass, respectively. The estimated intermolecular vibrational amplitude in a vacuum (vibrational quantum number being zero) and the thermal state are estimated to be 0.016 and  $0.023\text{ \AA}$ , respectively. The amplitude ( $0.09\text{ \AA}$ ) estimated for the vibration induced by the ultrashort pulse in the present study is thus larger than these and hence could clearly be observed.

### 3.4. Effect of Molecular Vibration on Transition Energy.

The modulation of normalized transmittance change can not only be due to absorbance modulation but also due to energy shift. To discuss on this, the eigenstates of the dimer interaction between the ground state, charge resonance (CR) states, and exciton coupling (EC) states are to be considered. As previously described, even with CR interaction only, the two-level systems composed of the ground state and CT state in each component molecule in the dimer become a four-level system. In the same way, a dimer system with interaction only between the ground state and EC states becomes a four-level system. Since we are considering the CR states, we can take into account only the CR coupling for the discussion of energy shift. This situation is different from the situation of the transition moment since in the latter case the transition moment is borrowed from the transition moment from the ground state to the locally excited state as discussed before.

If we disregard the interaction between the CT states and the ground state and that between the CT state and LE states, the energy of the CT states can be given by the following equation:

$$E_{CT}^A = I - A - C(\theta_A; \phi_B) \quad (31)$$

Here  $I$  and  $A$  are the ionization potential and electron affinity of a SnPc molecule. The last term  $C(\theta_A; \phi_B)$  in eq 31 is the Coulombic interaction given by the following equation:

$$C(\theta_A; \phi_B) = \int \theta_A^*(1) \theta_A(1) \frac{e^2}{V_2} \phi_B^*(2) \phi_B(2) d\tau_1 d\tau_2 \quad (32)$$

The off-diagonal terms of CT configuration with the ground and the LE states are given by

$$\langle G|H|CT^A \rangle = \sqrt{2} \langle \theta_A | H^c | \phi_B \rangle \quad (33)$$

$$\langle LE^A | H | CT^A \rangle = d_{LE} C_{CT} \langle \theta_A | H^c | \theta_B \rangle \quad (34)$$

Here  $H^c$  is the core attraction term of the total electronic Hamiltonian of the system. The integral is assumed to be proportional to the overlap integral as follows:

$$\langle \theta_A | H^c | \phi_B \rangle = -KS_{\theta_A \phi_B} \quad (35)$$

The size of the derivative contribution is 25% of total modulation and by comparing with derivative in eq 27  $\delta E_{CR}$  was estimated to be  $240\text{ meV}$  ( $190\text{ cm}^{-1}$ ), which is in fair agreement with the above value determined. Since the contribution of the off-diagonal to the transition energy is much smaller than the diagonal term of eq 31, the term is expected to be small. In comparison with the transition moment, which is directly proportional to the overlap in eq 28, the effect of the change in the overlap integral associated with the molecular vibration is only a small fraction. The total transition energy to the  $CT^A$  state is given as follows:

$$E_{CTA}^r = I - A - C(\theta_A; \phi_B) + D \quad (36)$$

Here  $I$  and  $A$  are the ionization potential and electron affinity

of a Pc molecule, and  $D$  is the contribution of the off-diagonal proportional to the squared overlap integral. Since  $I$  and  $A$  represent the intrinsic properties of molecule, they are not modulated by intermolecular vibration. Assuming that  $E_{\text{CTA}}^{\text{tr}}$  being the observed CR transition energy  $E_{\text{CR}} = 2.06$  eV and  $I = 6.5$  eV,  $A = 1.5$  eV, and  $C = 3$  eV,  $D$  is estimated to be 75 meV. The Coulombic energy change due to distance modulation during molecular vibration is estimated to be 2.5% because the previously estimated distance variation is 2.5%.

$$\left| \frac{\delta C}{C} \right| = \left| \frac{\delta(1/r)}{1/r} \right| = \left| \frac{\delta r}{r} \right| \quad (37)$$

Then  $\delta C$  is estimated as  $75 \text{ meV} = 600 \text{ cm}^{-1}$ . Previously estimated  $\delta E_{\text{CR}}$  from the molecular amplitude spectrum of CR band in comparison with the energy derivative of the CR band is  $190 \text{ cm}^{-1}$ . Therefore  $\delta D$  is estimated as  $410 \text{ cm}^{-1}$  and  $\delta E_{\text{CR}}/E_{\text{CR}}$  is as small as about  $1.1 \times 10^{-2}$ .

#### 4. Conclusion

In conclusion, we analyzed the modulation of the absorbance change in the bleaching spectral range of CR absorption band. The modulation can be explained in terms of periodical change in the cross section and periodical energy shift of the CR transition. Both are induced by the change in the overlap integral caused by the accordion-type intermolecular vibration. The size of the change in the intermolecular distance was estimated to be  $0.09 \text{ \AA}$ . The change of the transition energy due to the modulations of Coulombic interaction and wave function overlap was 75 meV.

**Acknowledgment.** This research is partly supported by the Grant-in-Aid for Specially Promoted Research (JSPS-GASR-14002003) from the Ministry of Education, Culture, Sports, Science and Technology, Japan, and also partly by the program for the "Promotion of Leading Researches" in Special Coordination Funds for Promoting Science and Technology from the Ministry of Education, Culture, Sports, Science and Technology.

#### References and Notes

(1) Coulson, C. A. *Valence*; Oxford University Press: London, New York, 1961.

- (2) Tokura, Y.; Koda, T.; Iyechika, Y.; Kuroda, H. *Chem. Phys. Lett.* **1983**, *102*, 174.
- (3) Keller, H. J. In *Extended Linear Chain Compounds*; Miller, J. S., Ed.; Plenum: New York, 1983; Vol. 1, p 357.
- (4) Birks, J. B. In *Organic Molecular Photophysics*; Birks, J. B.; McGlynn, S. P., Eds; John Wiley & Sons: London, 1975; Vol. 2, p 494.
- (5) Iyechika, Y.; Yakushi, K.; Ikemoto, I.; Kuroda, H. *Acta Crystallogr.* **1982**, *38*, 766.
- (6) Nalwa, H.; Shirk, J. S. In *Phthalocyanines: Properties and Applications*; Leznoff, C. C.; Lever, A. B. P., Eds.; VCH: New York, 1996; Vol. 4, p 79.
- (7) Imanishi, Y.; Ishihara, S.; Hamada, T. *Mol. Cryst. Liq. Cryst.* **1998**, *315*, 111. Imanishi, Y.; Ishihara, S. *Thin Solid Films* **1998**, *331*, 309.
- (8) Jennings, C.; Aroca, R.; Hor, A.; Loutfy, R. O. *Spectrochim. Acta* **1985**, *41*, 1095.
- (9) Mizoguchi, K.; Mizui, K.; Kim, D. G.; Nakayama, M. *Jpn. J. Appl. Phys.* **2002**, *41*, 6421.
- (10) Hirasawa, M.; Sakazaki, Y.; Hane, H.; Kobayashi, T. *Chem. Phys. Lett.* **2004**, in press.
- (11) Kobayashi, T.; Saito, T.; Ohtani, H. *Nature* **2001**, *414*, 531.
- (12) Baltuška, A.; Fuji, T.; Kobayashi, T. *Opt. Lett.* **2002**, *27*, 306.
- (13) Kobayashi, T.; Shirakawa, A.; Matsuzawa, H.; Nakanishi, H. *Chem. Phys. Lett.* **2000**, *321*, 385.
- (14) Shirakawa, A.; Sakane, I.; Kobayashi, T. *Opt. Lett.* **1998**, *23*, 1292.
- (15) Williams, V. S.; Mazumdar, S.; Armstrong, N. R.; Ho, Z. Z.; Peyghambarian, N. *J. Phys. Chem.* **1992**, *96*, 4500.
- (16) Kobayashi, T.; Fuji, T.; Ishii, N.; Goto, N. *J. Lumin.* **2001**, *94*–95, 667.
- (17) Basova, T. V.; Kolesov, B. A. *J. Struct. Chem.* **2000**, *41*, 770.
- (18) Ishikawa, N.; Ohno, O.; Kaizu, Y.; Kobayashi, H. *J. Phys. Chem.* **1992**, *96*, 8832.
- (19) Ohno, O.; Ishikawa, N.; Matsuzawa, H.; Kaizu, Y.; Kobayashi, H. *J. Phys. Chem.* **1989**, *93*, 1713.
- (20) Iwata, S.; Tanaka, J.; Nagakura, S. *J. Am. Chem. Soc.* **1967**, *89*, 2813. Iwata, S.; Tanaka, J.; Nagakura, S. *J. Am. Chem. Soc.* **1966**, *88*, 894. Kobayashi, T.; Iwata, S.; Nagakura, S. *Bull. Chem. Soc. Jpn.* **1970**, *43*, 713.
- (21) Mulliken, R. S. *J. Chem. Phys.* **1963**, *61*, 20.
- (22) Nitzan, A.; Jortner, J. *J. Chem. Phys.* **1972**, *56*, 3360. Henneker, W. H.; Siebrand, W.; Zgierski, M. Z. *Chem. Phys. Lett.* **1979**, *68*, 5. Siebrand, W.; Zgierski, M. Z. *Chem. Phys. Lett.* **1980**, *72*, 411. Siebrand, W.; Zgierski, M. Z. *J. Chem. Phys.* **1980**, *72*, 1641.
- (23) Henneker, H.; Siebrand, W.; Zgierski, M. Z. *J. Chem. Phys.* **1981**, *74*, 6560. Lu, H. M.; Page, J. B. *J. Chem. Phys.* **1988**, *88*, 3508. Albrecht, A. C.; Clark, R. J., H.; Oprescu, D.; Owens, S. J. R.; Svendsen, C. *J. Chem. Phys.* **1994**, *101*, 1809.
- (24) Franzen, S.; Goldstein, R. F.; Boxer, S. G. *J. Phys. Chem.* **1993**, *97*, 3040.
- (25) Goto, H.; Adachi, Y.; Ikoma, T. *Phys. Rev. B* **1980**, *22*, 782. Tanimura, Y.; Mukamel, S. *J. Opt. Soc. Am. B* **1993**, *10*, 2263.
- (26) Kano, H.; Saito, T.; Kobayashi, T. *J. Phys. Chem. A* **2002**, *106*, 3445. Kano, H.; Saito, T.; Kobayashi, T. *J. Phys. Chem. B* **2001**, *105*, 413.